JOURNAL OF Applied Polymer SCIENCE

Heterogeneous hydrolytic degradation of poly(lactic-*co*-glycolic acid) microspheres: Mathematical modeling

Carlos Busatto, Juan Pesoa, Ignacio Helbling, Julio Luna, Diana Estenoz
Instituto de Desarrollo Tecnológico para la Industria Química, INTEC (Universidad Nacional del Litoral and CONICET), Güemes 3450, Santa Fe 3000, Argentina
Correspondence to: D. Estenoz (E-mail: destenoz@santafe-conicet.gov.ar)

ABSTRACT: A new mathematical model for the prediction of the heterogeneous hydrolytic degradation of poly(D,L-lactide-*co*-glycolide) (PLGA)-based microspheres was developed. The model takes into account the autocatalytic effect of carboxylic groups and polymer composition on the degradation rate. It is based on mass balances for the different species, considering the kinetic and mass transport phenomena involved. The model estimates the evolution of average molecular weight, mass loss, and morphological change of the particles during degradation, and it was validated with novel experimental data. Theoretical predictions are in agreement with the hydrolysis data of PLGA microspheres (error values less than 5%). The model is able to predict the effect of particle size and molecular weight on the degradation of PLGA-based microspheres and estimates the morphological changes of the particles due to the autocatalytic effect. © 2017 Wiley Periodicals, Inc. J. Appl. Polym. Sci. 000: 000–000, 2017

KEYWORDS: biodegradable; degradation; drug-delivery systems; theory and modeling

Received 17 March 2017; accepted 26 June 2017
DOI: 10.1002/app.45464

INTRODUCTION

Microspheres prepared from poly(D,L-lactide-*co*-glycolide) (PLGA) have been studied extensively as drug-delivery systems.[1–4] Controlled or sustained drug-release systems have several advantages compared with conventional administration forms: reduced side effects, drug concentration at maintained effective levels in plasma, improved drug utilization, and decreased dosage times.[5] In pharmaceutical and biomedical applications, biodegradable microspheres are preferred because additional surgery to remove the drug-delivery system is avoided. Among biodegradable polymers, PLGA is widely used because it is approved by the U.S. Food and Drug Administration and the European Medicine Agency for parenteral use, and it has suitable degradation characteristics and possibilities for sustained drug delivery. It is possible to control the degradation time of the polymeric matrix by modifying several parameters, such as polymer molecular weight, lactide-to-glycolide ratio, and drug concentration, in order to achieve a desired dosage based on the drug type.[6–8]

Several processes affect the drug-release kinetics from PLGA microspheres, including polymer degradation by autocatalytic hydrolysis, polymer erosion, pore structure evolution, and diffusive transport of the drug through the polymeric matrix.[9] As mentioned, degradation plays a major role in the drug-delivery process from PLGA microspheres. Being a polyester, PLGA is hydrolytically cleaved into shorter chains with alcohol and acid groups.[10] As PLGA-based microparticles undergo bulk degradation, oligomers with acid groups are generated throughout the particles and diffuse out into the surrounding medium. In addition, bases from the bulk fluid diffuse into the microparticles, neutralizing the generated acids. However, diffusional mass transport is relatively slow, especially in polymer-based matrixes.[11] Thus, the rate at which the acids are generated within the microparticles can be higher than the rate at which they are neutralized, lowering the pH of the system. Several studies using indirect methods have shown the presence of an acidic environment within degrading PLGA devices.[12–14]

The drop in the internal pH promotes further polymer degradation because the ester bond cleavage is catalyzed by protons. With increasing microparticle size, the diffusion pathways for the species increases. Thus, diffusion rates decrease, and the drop in micro-pH and acceleration of polymer degradation become more pronounced. This is especially important in the center of the microparticles because the diffusion pathways are the longest, leading to heterogeneous degradation.[15] In addition, during degradation, mass loss occurs due to diffusion of water-soluble oligomers and monomers out of the polymeric matrix.

Mathematical models are an important tool in biomedical science because they can be used to design or optimize novel drug-delivery systems in accordance with the requirements for composition, geometry, dimensions, and release profile. Thus, it is possible to significantly reduce the number of required experimental studies during

J_ID: z8e Customer A_ID: APP45464 Cadmus Art: APP45464 Ed. Ref. No.: 20170772 Date: 7-July-17 Stage: Page: 2

device development, saving time and reducing costs. In this direction, several kinetic models have been proposed for polymer degradation, including pseudo-first-order kinetics,[10,16] 1.5th-order kinetics with partial dissociation of —COOH groups,[17] second-order kinetics,[18–20] and 2.5th-order kinetics.[21] Nishida *et al.*[20] used moment analysis to predict changes in average molecular weight of aliphatic polyesters subject to autocatalytic random hydrolysis. The model successfully interpreted the hydrolysis data of aliphatic polyester films. Wang *et al.*[22] developed a phenomenological model that is able to predict the degradation of polylactic acid plates of different thickness based on a set of simplified diffusion–reaction equations. The model considers hydrolysis reactions and monomer diffusion and accurately predicts the decrease of average molecular weight. Han and Pan[23] extended the model of Wang *et al.*[22] in order to include the interplay between the crystallization degree and hydrolysis reaction during degradation. The model simulates the evolution of average molecular weight, degree of crystallinity, and weight loss of biodegradable films. Soares and Zunino[24] also proposed a mixed model to describe water-dependent degradation and both bulk and surface erosion of biodegradable polymers by solving a system of reaction–diffusion equations. Antheunis *et al.*[18] proposed a kinetic model based on the autocatalytic hydrolysis of aliphatic polyester rods. The model describes the decrease of average molecular weights in an accurate way, and it is also able to reasonably predict the mass loss trend of the polymer through coupled ordinary differential equations. The model was then simplified to predict the number-average molecular weight (M_n) without the need for complicated mathematics and excessive input parameters.[19] Chen *et al.*[25] developed a model for bulk-eroding polymers that allows the prediction of the time evolution of average molecular weight and estimates the mass loss for various device geometries. This model considers autocatalysis and monomer diffusion, with a degradation-dependent diffusivity. Casalini *et al.*[26] described the degradation of PLGA microparticles through mass-conservation equations. The model takes into account the oligomer diffusion and autocatalytic effects, and it is able to predict the decrease of average molecular weights for microparticles of different sizes.

In our previous work, a mathematical model that simulates the homogeneous degradation of PLGA microspheres was developed.[27] The model takes into account the autocatalytic effect of carboxylic groups and polymer composition on the polymer degradation rate, and it is based on a detailed kinetic mechanism that considers the hydrolysis of the different types of ester bonds in the copolymer by random chain scission. In spite of the mentioned publications, the mathematical modeling of the autocatalytic heterogeneous degradation of PLGA microspheres has not been extensively described in terms of polymer composition, molecular weight distribution, mass loss, and morphological structure of the particle during degradation. The estimation of these profiles allows us to better understand the degradation process and to study the effect of formulation parameters on the degradation behavior.

The aim of the present work is to develop a mathematical model for the heterogeneous degradation of PLGA-based microspheres. The model takes into account the autocatalytic effect of carboxylic groups and polymer composition on the degradation rate, and it is based on mass balances for the different species considering the kinetic and mass-transport phenomena involved. The model predicts the following evolutions along degradation: (1) radial profile of average molecular weights and molecular weight distributions, (2) mass loss, and (3) morphological structure of the particle. In order to validate the model, PLGA microparticles of different sizes were prepared and characterized, and their degradation in a phosphate-buffered saline buffer was studied. The model can be used to study the effect of particle size and molecular weight of the polymer on the degradation rate, in order to design an appropriate polymeric particle system to achieve a desired degradation time.

EXPERIMENTAL

PLGA microparticles were prepared by the solvent extraction/evaporation technique. Degradation experiments of different-sized microspheres were performed in a phosphate-buffered saline buffer, and polymeric microparticles were characterizated by optical and scanning electron microscopy (SEM), size exclusion chromatography (SEC), and gravimetric measurements.

MATERIALS

Poly(D,L-lactide-*co*-glycolide) 50:50, with weight-average molecular weight (M_w) of 6622 Da (Shanghai Easier Industrial Development Co., Shanghai, China), HPLC-grade tetrahydrofurane (THF; Merck, Darmstadt, Germany), methylene chloride (Ciccarelli, San Lorenzo, Argentina), polyvinyl alcohol (PVA; 205 kDa; 87.7% hydrolyzed; Sigma Aldrich, Saint Louis, United States), sodium hydrogen phosphate (Na_2HPO_4; Anedra, Buenos Aires, Argentina), and potassium dihydrogen phosphate (KH_2PO_4; Anedra) were used as received. Distilled and deionized water was used to prepare all of the solutions.

Microsphere Preparation

A solvent extraction/evaporation technique was used for microsphere preparation.[28] Briefly, 450 mg of PLGA was dissolved in 3 mL of methylene chloride, and the solution was added dropwise into the stirred aqueous phase (2% w/v PVA solution, 17 mL) using an Ultra-Turrax T25D homogenizer (dispersing element S25N-18G, IKA, Staufen, Germany). The oil-in-water emulsion was stirred for 5 min at different rpm in order to obtain microparticles of different sizes. Then, 70 mL of 0.3% w/v PVA solution was added, and the dispersion was stirred for 30 min. The remaining organic solvent was evaporated using a rotary evaporator under vacuum (400 mbar) for 3 h at room temperature. Solid microspheres were washed three times with deionized water and collected by centrifugation. Finally, the particles were lyophilized and stored for further assays.

Degradation Studies

Glass vials containing 40 mg of dry microspheres and 10 mL of phosphate buffer (1 m*M*, pH 7.4) were prepared for each sample. Vials were orbitally shaken at 50 rpm in an oven with digital temperature control at 37.0 ± 0.5 °C. At different times, the degradation medium was removed, and the microsphere sample was dried under vacuum at room temperature and used for the characterization analysis.

Characterization

Microsphere Size Distribution Determination. The microsphere samples were resuspended in distilled water and observed with an optical microscope (DM 2500M, Leica, Wetzlar, Germany) coupled with a Leica DM 2500M DFC 290HD camera.

ID: jwweb3b2server Time: 13:01 I Path: D:/Wiley/Support/XML_Signal_Tmp_AA/JW-APP#170615

J_ID: z8e Customer A_ID: APP45464 Cadmus Art: APP45464 Ed. Ref. No.: 20170772 Date: 7-July-17 Stage: Page: 3

Microsphere diameters and particle size distributions were determined by analyzing photomicrographs with an image processing program. An average of 300 particles per sample were observed for diameter determination.

Mass Loss Determination. During the degradation study, samples were collected by centrifugation, and the remaining mass was vacuum-dried up to constant weight. The polymer mass loss was determined gravimetrically using eq. (1):

$$\%\ \text{Mass loss} = \frac{w_t}{w_0} \times 100 \tag{1}$$

where w_0 is the initial dry weight of microspheres, and w_t is the dry weight after incubation at time t.

Polymer Molecular Weight Determination. The average molecular weights of the samples were determined by size exclusion chromatography (SEC) using a Waters-Breeze, Milford, United States, liquid chromatograph equipped with a Waters Styragel column (HR 4E, 7.8 mm × 300 mm), a pump (Waters 1525), and a refractive index detector (Waters 2414). The carrier solvent was tetrahydrofuran at a flow rate of 1.0 mL min^{-1}. Polystyrene standards (Shodex SM-105, Showa Denko, Kawasaki, Japan) were used for calibration.

Morphology Studies. The morphology of the microsphere samples was studied by scanning electron microscopy. Samples were put over an aluminum stub and were then sputter-coated with gold under argon atmosphere (12157-AX, SPI Supplies, West Chester, United States) using soft conditions (two sputterings of 40 s each with an intensity of 15 mA). The morphology of the microparticles was examined using an acceleration voltage of 20 kV in a JEOL, Tokyo, Japan, JSM-35C SEM equipped with the image acquisition program JEOL SemAfore.

Oligomer Dissolution Study. The molecular weight of the water-soluble degradation products was determined by size exclusion chromatography using a Waters-Breeze liquid chromatograph equipped with a Waters Ultrahydrogel 120 column (7.8 mm × 300 mm), a pump (Waters 1525), and a refractive index detector (Waters 2414). The carrier phase was a phosphate buffer (0.1 m*M*, pH 7.4) at a flow rate of 0.8 mL min^{-1}. Polyethylene glycol standards (PPS Polymer Standards Service GmbH, Mainz, Germany) were used for calibration.

Mathematical Modeling

A mathematical model to predict the heterogeneous autocatalytic degradation of PLGA microspheres was developed on the basis of a kinetic mechanism that includes the hydrolysis of the different types of ester bonds by random chain scission. The model takes into account the autocatalytic effect of carboxylic groups and the effect of polymer composition on the degradation rate.

The general equation for the acid-catalyzed hydrolysis reaction can be expressed as follows:

$$\mathrm{P}_n + \mathrm{H_2O} \xrightarrow{\mathrm{H^+}} \mathrm{P}_r + \mathrm{P}_{n-r}; \quad n=1,2,3,\ldots; \quad r=0,1,2,\ldots(n-1) \tag{2}$$

where P_n and P_r are polymer chains of length n and r, respectively, and $\mathrm{H^+}$ is the acid catalyst. Polymer degradation generates shorter chains containing alcohol and acid groups, denoted as COOH and OH, respectively. The following global dissociation equilibrium can be written for acid groups:

$$\mathrm{COOH} \rightleftarrows \mathrm{COO^-} + \mathrm{H^+} \tag{3}$$

Following our previous work,[27] eq. (2) can be extended to consider the different types of species and the hydrolysis of different ester groups:

$$\mathrm{P}_n(l,g,c) + H_2O \xrightarrow{k_{L-L}} P_{n-m}(l-l'-1, g-g', c-c') + P_m(l',g',c'); \quad \begin{array}{l} n=1,2,3,\ldots \\ l,g,c=0,1,2,3,\ldots \\ l'=0,1,2,3,\ldots,(l-1) \\ g'=0,1,2,3,\ldots,g \\ c'=0,1,2,3,\ldots,c \end{array} \tag{4}$$

$$\mathrm{P}_n(l,g,c) + H_2O \xrightarrow{k_{G-G}} P_{n-m}(l-l', g-g'-1, c-c') + P_m(l',g',c'); \quad \begin{array}{l} n=1,2,3,\ldots \\ l,g,c=0,1,2,3,\ldots \\ l'=0,1,2,3,\ldots,l \\ g'=0,1,2,3,\ldots,(g-1) \\ c'=0,1,2,3,\ldots,c \end{array} \tag{5}$$

$$\mathrm{P}_n(l,g,c) + H_2O \xrightarrow{k_{L-G}} P_{n-m}(l-l', g-g', c-c'-1) + P_m(l',g',c'); \quad \begin{array}{l} n=1,2,3,\ldots \\ l,g,c=0,1,2,3,\ldots \\ l'=0,1,2,3,\ldots,l \\ g'=0,1,2,3,\ldots,g \\ c'=0,1,2,3,\ldots,(c-1) \end{array} \tag{6}$$

ID: jwweb3b2server Time: 13:01 I Path: D:/Wiley/Support/XML_Signal_Tmp_AA/JW-APP#170615

J_ID: z8e Customer A_ID: APP45464 Cadmus Art: APP45464 Ed. Ref. No.: 20170772 Date: 7-July-17 Stage: Page: 4

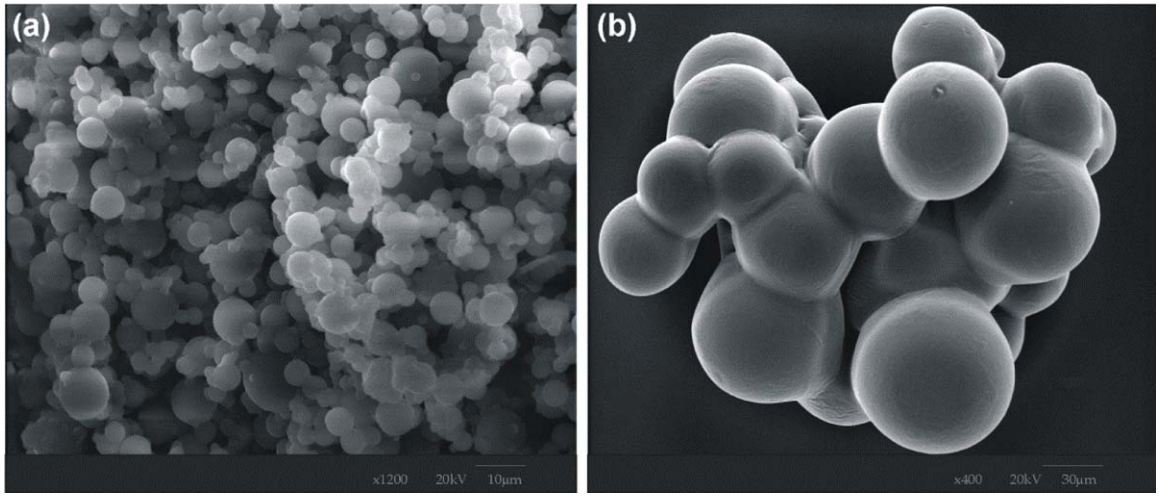

Figure 1. SEM photographs of PLGA-based microspheres with different diameters: (a) average diameter: 8.94 ± 3.30 μm; (b) average diameter: 52.37 ± 17.73 μm. [Color figure can be viewed at wileyonlinelibrary.com]

In eqs. (4)–(6), polymer species are characterized by their chain length and by the number of each ester bond type. The following nomenclature is adopted: $P_n(l, g, c)$ represents a polymer chain of length n with l, g, and c, lactic-lactic (L-L), glycolic-glycolic (G-G), and lactic-glycolic (L-G) ester bonds, respectively; and $k_{L\text{-}L}$, $k_{G\text{-}G}$, and $k_{L\text{-}G}$ are the hydrolysis constants corresponding to the L-L, G-G, and L-G ester bonds, respectively.

From the kinetics of eqs. (2)–(6) and considering the radial mass transport of species, the mathematical model described in the Appendix was derived. The model assumes the following hypotheses: (1) hydrolysis rate constants are independent of chain length; (2) ester bonds are uniformly distributed inside the polymer chain; (3) all particles have the same size (represented by their mean diameter) and are modeled as a sphere of constant volume; (4) the polymer is totally amorphous; (5) oligomer species with a chain length up to n_s can be dissolved, n_s being the critical chain length for oligomer dissolution[29]; (6) the volume of degradation medium largely exceeds the microparticle volume; and (7) the generation rate of acid catalyst (H^+) within microparticles is higher than the diffusion rate.[18] Also, in order to quantify the mass transport, the variation of the diffusion coefficient with the weight-average molecular weight is considered.

The mathematical model was implemented in a Matlab routine. The model consists of a set of partial differential equations solved by using a finite difference scheme to discretize the radial dimension and a Forward Euler method for time discretization. The typical computing time in an Intel Core 2 Duo processor ranged between 1 and 3 min per simulation.

The model was adjusted and validated with the experimental data. To this effect, the $k_{L\text{-}L}$, $k_{G\text{-}G}$, and k_a1 kinetic constants and the transport parameter k_D were simultaneously adjusted to fit the evolution of M_n, M_w, and mass loss. Other parameters (K_a and D_{olig}°) were taken from the literature.

RESULTS AND DISCUSSION

Microspheres of two well-differentiated sizes were prepared by changing the stirring speed. Samples with average diameters of 8.9 ± 3.3 μm and 52.4 ± 17.7 μm were obtained with 4000 rpm and 500 rpm, respectively. SEM photographs of both samples are presented in Figure 1. Both formulations were spherical with smooth surfaces. However, larger microspheres presented higher polydispersity in particle size than the smaller ones. F1

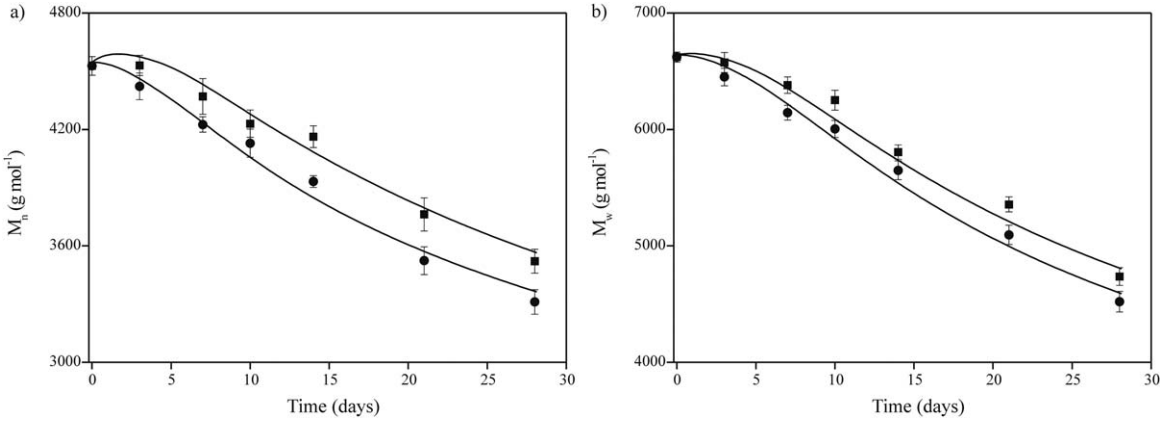

Figure 2. Evolution of average molecular weights during degradation of PLGA microparticles with different diameters: (■) 8.94 ± 3.30 μm, (●) 52.37 ± 17.73 μm, (–) model prediction; (a) number-average molecular weight (M_n); (b) weight-average molecular weight (M_w).

ID: jwweb3b2server Time: 13:01 I Path: D:/Wiley/Support/XML_Signal_Tmp_AA/JW-APP#170615

J_ID: z8e Customer A_ID: APP45464 Cadmus Art: APP45464 Ed. Ref. No.: 20170772 Date: 7-July-17 Stage: Page: 5

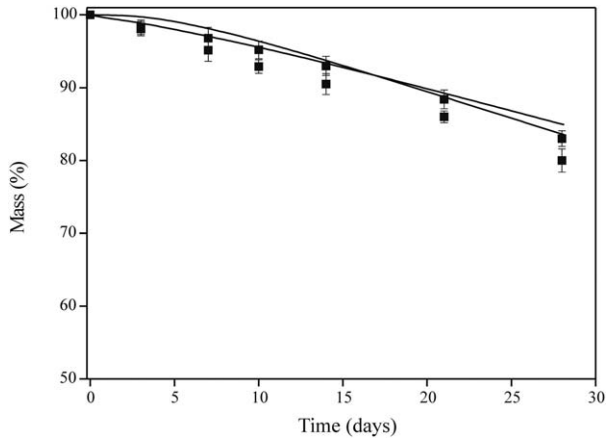

Figure 3. Evolution of mass loss during degradation of PLGA microparticles with different diameters: (■) 8.94 ± 3.30 μm, (●) 52.37 ± 17.73 μm, (–) model prediction.

Experimental data from the degradation studies are presented in F2 F3 Figures 2 and 3. Figure 2 shows the evolution of average molecular weights for both microsphere sizes. Three stages can be identified in the degradation profile. Initially the degradation proceeds slowly due to the low concentration of terminal carboxylic acid groups. Then, as degradation proceeds, the number of carboxylic acid groups increases and accelerates the hydrolysis reaction. Finally, the low concentration of ester bonds delays degradation. Also, it can be observed that microsphere degradation increases with particle size. The influence of particle size on the degradation is attributed to the fact that degradation products formed within smaller particles can diffuse easily to the particle surface, while in larger particles the length of the diffusion pathways increases. Therefore, degradation products are trapped within the particle and have the potential to catalyze the degradation of the remaining polymeric material.

Figure 3 shows the evolution of the remaining mass of microspheres during the degradation assays. As shown in Figure 3, the mass loss of the system increases with particle size. Low mass loss (<10%) was observed for both microsphere sizes during the first 5 days, and then it increased progressively. This can be explained by the fact that polymer must undergo sufficiently extensive degradation to produce water-soluble monomers and oligomers, so no reduction in mass is observed at the beginning of the degradation experiment. This observation has been reported previously in the literature.[30,31]

The mass loss is similar for both particle sizes at short times of degradation. However, although oligomers have longer diffusive paths as microsphere size increases, autocatalysis accelerates the degradation kinetics and therefore increases the particle porosity, enhancing the mass loss rate. The mean value of chain length at which oligomers can dissolve in the medium (n_s) is 16 repeat units, in accordance with experimental determinations by SEC (data not shown) and with reported data in similar experimental conditions.[29]

Figures 2 and 3 also present model theoretical predictions. As can be observed, the model is able to accurately predict the average molecular weight decrease during degradation, and hence the complete molecular weight distribution. Kinetic constants and transport parameters used for the simulations are listed in Table I. The hydrolysis constant $k_{L\text{-}G}$ was estimated T1 considering that it is a mean value between $k_{L\text{-}L}$ and $k_{G\text{-}G}$.[27] The direct and reverse acid dissociation constants k_{a1} and k_a2 are related by the equilibrium dissociation constant of carboxylic groups (K_a). Note that the cleavage rate of G-G bonds is faster than that of L-L bonds, consistent with experimental observations.[32,33] In addition, the k_D parameter depends on the particle size as a consequence of the variation of the porous structure, due to the catalytic effect.

The predicted and experimental mass loss profiles present some differences. It is possible that some systematic errors were introduced due to the determination method. During the removal of the buffer after degradation, a small amount of nondissolved polymer may have been removed by the syringe. This would give an increase in mass loss during the experiment. However, the mass loss is reasonably calculated, and the experimental trend is well predicted by the model developed. Therefore, it can be concluded that the model is able to describe the decrease of average molecular weight in an accurate way, and it is also able to reasonably predict the mass loss trend of the polymer.

The model was also used to simulate the evolution of molecular weight distribution and morphological structure of the particles during degradation (Figures 4 and 5) and to study the effect of F4 F5 experimental parameters on the degradation kinetics of the

Table I. Kinetic Constants and Transport Parameters

Parameter	Constant		Reference
$k_{L\text{-}L}$ (L mol^{-1} s^{-1})	2.55×10^{-7}		Adjusted in this work
$k_{G\text{-}G}$ (L mol^{-1} s^{-1})	1.27×10^{-6}		Adjusted in this work
$k_{L\text{-}G}$ (L mol^{-1} s^{-1})	7.63×10^{-7}		27
k_{a1} (s^{-1})	5.00×10^{-8}		Adjusted in this work
k_{a2} (s^{-1}) = $k_{a1}K_a$ ($K_a = 3.38 \times 10^{-4}$)	1.48×10^{-4}		34
$D_{olig}°$ (cm^2 s^{-1})	1.00×10^{-14}		22,35
k_D	4.00×10^{1} [a]	7.00×10^{2} [b]	Adjusted in this work

[a] Average diameter 8.94 ± 3.30 μm.
[b] Average diameter 52.37 ± 17.73 μm.

ID: jwweb3b2server Time: 13:01 I Path: D:/Wiley/Support/XML_Signal_Tmp_AA/JW-APP#170615

J_ID: z8e Customer A_ID: APP45464 Cadmus Art: APP45464 Ed. Ref. No.: 20170772 Date: 7-July-17 Stage: Page: 6

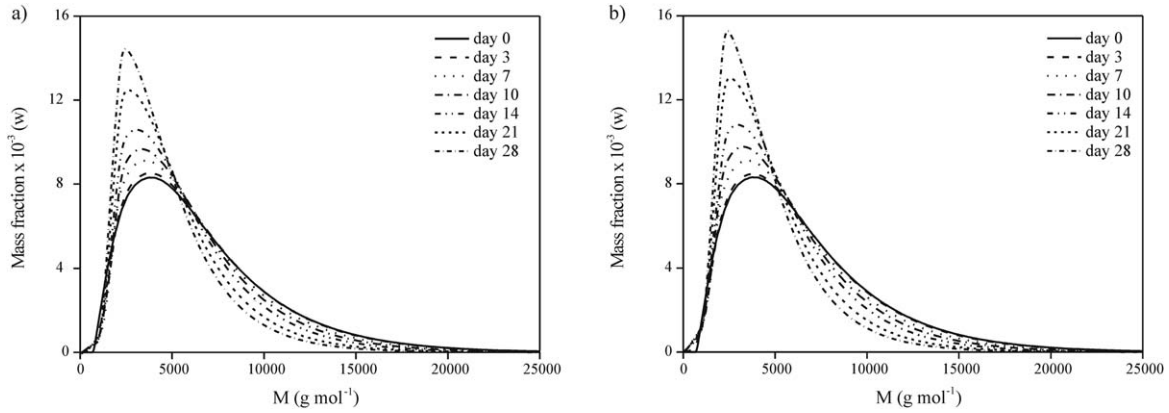

Figure 4. Predicted molecular weight distributions along degradation time: (a) 8.94 ± 3.30 μm PLGA microparticles; (b) 52.37 ± 17.73 μm PLGA microparticles.

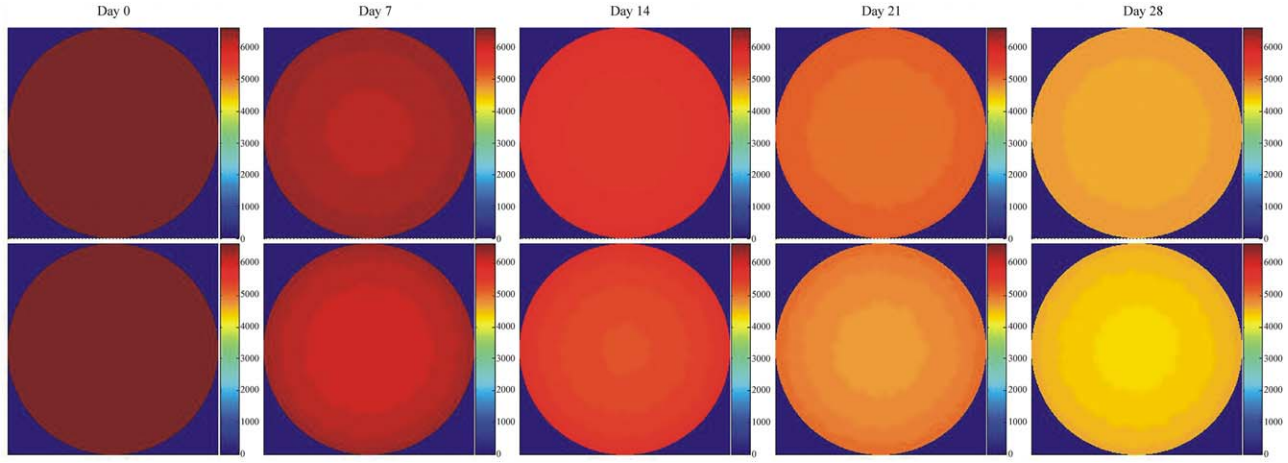

COLOR ONLINE AND BW IN PRINT

Figure 5. Predicted radial average molecular weight profiles inside microparticles during degradation: (top row) 8.94 ± 3.30 μm PLGA microparticles; (bottom row) 52.37 ± 17.73 μm PLGA microparticles. [Color figure can be viewed at wileyonlinelibrary.com]

F6 F7 microspheres (Figures 6 and 7). The theoretical evolution of molecular weight distribution (MWD) with degradation time for both microsphere sizes is shown in Figure 4. As expected, the MWDs shift toward lower molecular weights as degradation time proceeds. This shift increases with particle size, due to catalytic effects.

The predicted radial average molecular weight profiles inside microparticles (diameters 8.9 and 52.4 μm) during degradation are shown in Figure 5 and indicate the nonuniform degradation. The acumulation of degradation products with carboxylic groups inside the polymeric matrix encourages autocatalysis, leading degradation to proceed more rapidly in the center than

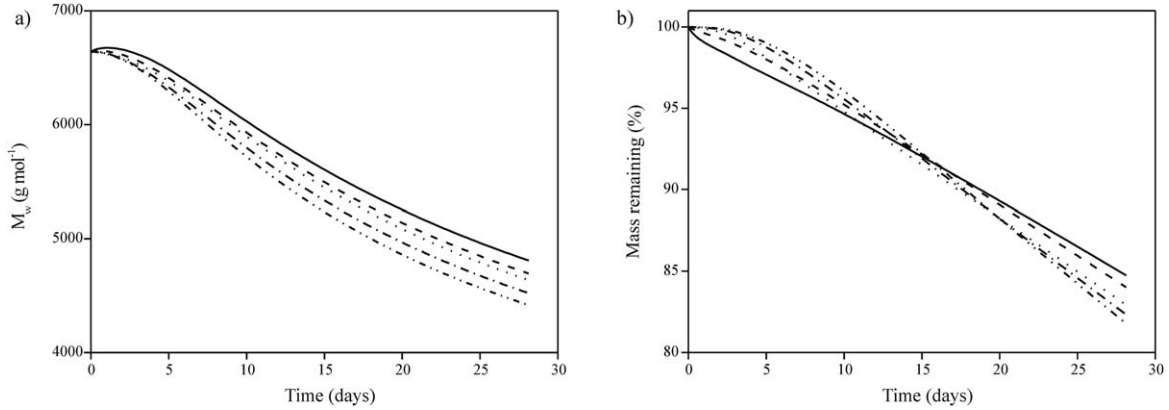

Figure 6. Theoretical effect of particle size on the degradation of PLGA microparticles: (a) predicted evolution of weight-average molecular weight; (b) predicted evolution of mass loss: (–) 5 μm, (---) 10 μm, (···) 25 μm, (-·-·) 50 μm, (-··-) 75 μm.

ID: jwweb3b2server Time: 13:01 I Path: D:/Wiley/Support/XML_Signal_Tmp_AA/JW-APP#170615

J_ID: z8e Customer A_ID: APP45464 Cadmus Art: APP45464 Ed. Ref. No.: 20170772 Date: 7-July-17 Stage: Page: 7

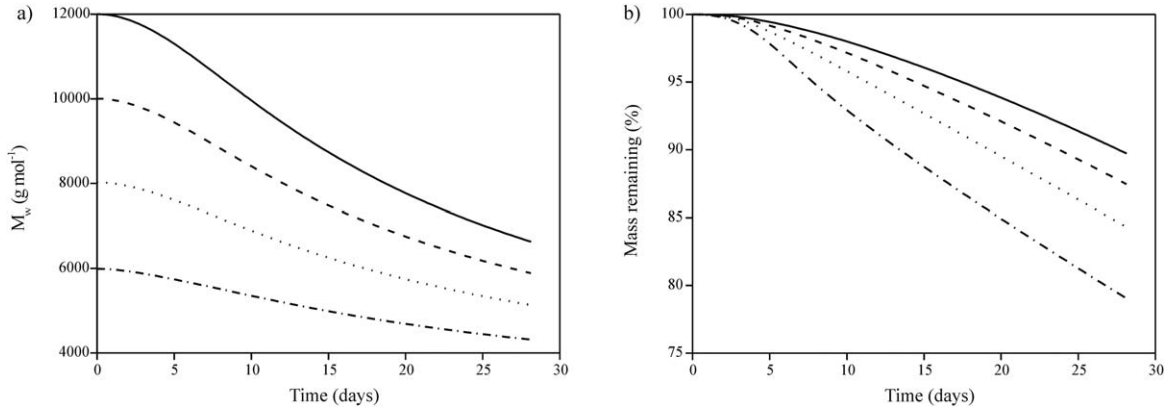

Figure 7. Theoretical effect of the initial molecular weight on the degradation of PLGA microparticles with a diameter of 52.4 μm: (a) predicted evolution of weight-average molecular weight; (b) predicted evolution of mass loss: (-···-) 6000 g mol^{-1}, (-···-) 8000 g mol^{-1}, (---) 10,000 g mol^{-1}, (–) 12,000 g mol^{-1}.

at the surface. As can be observed, this effect becomes more important as the particle size increases, due to the longer diffusion path. Note that there are other factors related to this type of degradation, such as the porosity of the particles, the particle size, the initial terminal groups in the polymer, and the polymer molecular weight.

Figure 6 presents the predicted evolution of weight-average molecular weight and mass loss for microparticles of different sizes. The polymer degradation becomes more pronounced with increasing microparticle dimension. The length of the diffusion pathways for the acidic degradation products increases with microparticle size, leading to a faster decrease in the microenvironmental pH, and thus ester bond cleavage is accelerated. The mass loss increases faster for smaller microparticles at short times of degradation because they have more surface area. However, the mass loss for larger particles is higher as degradation proceeds because the autocatalytic effects become more important with increasing particle size. The theoretical prediction trends are in agreement with experimental data reported earlier.[10,36]

Figure 7 shows the predicted evolution of weight-average molecular weight and mass loss for 52.4 μm microparticles as a function of the PLGA initial molecular weight. In agreement with published data,[37] it can be observed that the molecular weight decreases faster for higher initial molecular weights due to the accumulation of acidic degradation products within the particles, which also promotes autocatalysis. The mass loss increases for lower initial molecular weights due to the rapid generation of monomers and oligomers, which can diffuse away from the microspheres into the surrounding media.

CONCLUSIONS

A mathematical model to predict the heterogeneous hydrolytic degradation of PLGA microspheres was developed. The model allows us to estimate the evolution of average molecular weight, molecular weight distribution, and mass loss of the microparticles during the degradation time. The theoretical results are in agreement with experimental measurements (error values less than 5%). In addition, the model was able to predict the morphological changes of different-sized microparticles during degradation, and it was used to study the effect of particle size and molecular weight on the degradation of PLGA microparticles. The model can be used to design an appropriate drug-delivery particle system with a prespecified degradation time. In future works, the model will be extended to predict the controlled release of drugs from PLGA microparticles.

APPENDIX

From eqs. (4)–(6) and considering constant volume, the following mass balances for each P_n species are derived:

$$\frac{\partial \sum_{l=0}^{\infty}\sum_{g=0}^{\infty}\sum_{c=0}^{\infty}[P_n]}{\partial t} = \frac{1}{r^2}\frac{\partial}{\partial r}\left(r^2 D_{P_n}\frac{\partial \sum_{l=0}^{\infty}\sum_{g=0}^{\infty}\sum_{c=0}^{\infty}[P_n]}{\partial r}\right) - k_{L\text{-}L}\, l \sum_{l=0}^{\infty}\sum_{g=0}^{\infty}\sum_{c=0}^{\infty}[P_n][H^+] - k_{G\text{-}G}\, g \sum_{l=0}^{\infty}\sum_{g=0}^{\infty}\sum_{c=0}^{\infty}[P_n][H^+] - k_{L\text{-}G}\, c \sum_{l=0}^{\infty}\sum_{g=0}^{\infty}\sum_{c=0}^{\infty}[P_n][H^+]$$
$$+\sum_{l=0}^{\infty}\sum_{g=0}^{\infty}\sum_{c=0}^{\infty}\left\{\sum_{m=n+1}^{\infty}\left(\sum_{k=l+1}^{\infty} k_{L\text{-}L}\, p_k\, k[P_m(k,g,c)] + k_{G\text{-}G}\sum_{h=g+1}^{\infty} p_h\, h[P_m(l,h,c)] + \sum_{d=c+1}^{\infty} k_{L\text{-}G}\, p_d\, d[P_m(l,g,d)]\right)\right\}$$
$$n = 1, 2, 3, \ldots; \quad n < n_s \tag{A.1}$$

where n_s is the critical chain length for oligomer dissolution, D_{P_n} is the effective diffusivity of the polymer chains P_n, and r is the radial position within a microsphere. Note that the chain length n is related to the number of ester bonds as $n = l + g + c + 1$.

ID: jwweb3b2server Time: 13:01 I Path: D:/Wiley/Support/XML_Signal_Tmp_AA/JW-APP#170615

J_ID: z8e Customer A_ID: APP45464 Cadmus Art: APP45464 Ed. Ref. No.: 20170772 Date: 7-July-17 Stage: Page: 8

Considering $[P^-] = [H^+]$, the following mass balance for H^+ is derived:

$$\frac{d[H^+]}{dt} = k_{a_1}[P] - k_{a_2}[H^+]^2 \quad (A.2)$$

where [P] is the total concentration of polymer at each radial position, defined as

$$[P] = \sum_{n=1}^{\infty}\sum_{l=0}^{\infty}\sum_{g=0}^{\infty}\sum_{c=0}^{\infty}[P_n(l,g,c)] \quad (A.3)$$

Regarding boundary conditions, the symmetry condition for the concentration of oligomers is applied in the center of the microparticle:

$$\left.\frac{\partial[P_n]}{\partial r}\right|_{r=0} = 0 \quad n < n_s \quad (A.4)$$

In the microparticle–aqueous medium interface, a sink condition is considered:

$$\left.[P_n]\right|_{r=R} = 0 \quad n < n_s \quad (A.5)$$

The increase of diffusivity during degradation is related to the evolution of the weight-average molecular weight through the following expression[35]:

$$D_{P_n} = D^0_{P_n}\left[1 + \left(1 - \frac{\overline{M}_w(t,r)}{\overline{M}_w(t=0)}\right)(k_D - 1)\right] \quad n < n_s \quad (A.6)$$

where $D^0_{P_n}$ is the initial diffusivity of the polymer chains, $\overline{M}_w$ is the weight-average molecular weight, and k_D is an adjustment parameter related to the effective diffusivities of the species in aqueous solution and in the solid. This equation allows coupling of the evolution of the pore network to the effective diffusivity.

From eq. (A.1), the number chain length distribution (NCLD) of the copolymer can be estimated:

$$x_n = \frac{\int_0^R [P_n(l,g,c)]\ r^2\ dr}{\int_0^R \sum_{n=1}^{\infty}\sum_{l=0}^{\infty}\sum_{g=0}^{\infty}\sum_{c=0}^{\infty}[P_n(l,g,c)]\ r^2\ dr} \quad (A.7)$$

Multiplying eq. (A.7) by the average molecular weight of the repeating unit (M_{RU}), the weight chain length distribution (WCLD) can be calculated:

$$x_w = \frac{\int_0^R [P_n(l,g,c)]\ n\,M_{RU}\ r^2\ dr}{\int_0^R \sum_{n=1}^{\infty}\sum_{l=0}^{\infty}\sum_{g=0}^{\infty}\sum_{c=0}^{\infty}[P_n(l,g,c)]\ n\,M_{RU}\ r^2\ dr} \quad (A.8)$$

where $M_{RU} = x_{L\text{-}L}M_{L\text{-}L} + x_{G\text{-}G}M_{G\text{-}G} + x_{L\text{-}G}M_{L\text{-}G}$. In this equation, $M_{L\text{-}L}$, $M_{G\text{-}G}$, and $M_{L\text{-}G}$ are the molar masses of the corresponding ester repeating units, and $x_{L\text{-}L}$, $x_{G\text{-}G}$, and $x_{L\text{-}G}$ represent the molar fraction of L-L, G-G, and L-G ester bonds, given by

$$x_{L\text{-}L} = \frac{[E_{L\text{-}L}]}{[E_{L\text{-}L}] + [E_{G\text{-}G}] + [E_{L\text{-}G}]} \quad (A.9)$$

$$x_{G\text{-}G} = \frac{[E_{G\text{-}G}]}{[E_{L\text{-}L}] + [E_{G\text{-}G}] + [E_{L\text{-}G}]} \quad (A.10)$$

$$x_{L\text{-}G} = \frac{[E_{G\text{-}L}]}{[E_{L\text{-}L}] + [E_{G\text{-}G}] + [E_{L\text{-}G}]} \quad (A.11)$$

The copolymer average molecular weights are estimated as follows:

$$\overline{M}_n = \frac{\int_0^R \sum_{n=1}^{\infty}\sum_{l=0}^{\infty}\sum_{g=0}^{\infty}\sum_{c=0}^{\infty}[P_n(l,g,c)]\ n\,M_{RU}\ r^2\ dr}{\int_0^R \sum_{n=1}^{\infty}\sum_{l=0}^{\infty}\sum_{g=0}^{\infty}\sum_{c=0}^{\infty}[P_n(l,g,c)]\ r^2\ dr} \quad (A.12)$$

$$\overline{M}_w = \frac{\int_0^R \sum_{n=1}^{\infty}\sum_{l=0}^{\infty}\sum_{g=0}^{\infty}\sum_{c=0}^{\infty}[P_n(l,g,c)]\ (n\,M_{RU})^2\ r^2\ dr}{\int_0^R \sum_{n=1}^{\infty}\sum_{l=0}^{\infty}\sum_{g=0}^{\infty}\sum_{c=0}^{\infty}[P_n(l,g,c)]\ n\,M_{RU}\ r^2\ dr} \quad (A.13)$$

ACKNOWLEDGMENTS

The authors wish to express their gratitude to Consejo Nacional de Investigaciones Científicas y Técnicas (CONICET) and to Universidad Nacional del Litoral (UNL) of Argentine for the financial support granted to this contribution.

REFERENCES

1. Tang, J.; Liu, Z.; Zhang, Y.; Wang, L.; Li, D.; Ding, J.; Jiang, X. *RSC Adv.* **2015**, *5*, 30153.
2. Qi, F.; Wu, J.; Fan, Q.; He, F.; Tian, G.; Yang, T.; Ma, G.; Su, Z. *Colloids Surf., B* **2013**, *112*, 492.
3. Freiberg, S.; Zhu, X. X. *Int. J. Pharm.* **2004**, *282*, 1.
4. Varde, N. K.; Pack, D. W. *Expert Opin. Biol. Ther.* **2004**, *4*, 35.
5. Kim, B. K.; Hwang, S. J.; Park, J. B.; Park, H. J. *J. Microencapsulation* **2002**, *19*, 811.
6. Li, Z. H.; Wu, J. M.; Zhao, Y. L.; Guan, J.; Huang, S. J.; Li, R. X.; Zhang, X. Z. *Adv. Mater. Res.* **2012**, *466–467*, 405.
7. Zilberman, M.; Grinberg, O. *J. Biomater. Appl.* **2008**, *1*, 391.
8. Blanco, D.; Alonso, M. J. *Eur. J. Pharm. Biopharm.* **1998**, *45*, 285.
9. Fredenberg, S.; Wahlgren, M.; Reslow, M.; Axelsson, A. *Int. J. Pharm.* **2011**, *415*, 34.
10. Siepmann, J.; Elkharraz, K.; Siepmann, F.; Klose, D. *Biomacromolecules* **2005**, *6*, 2312.
11. Klose, D.; Siepmann, F.; Elkharraz, K.; Krenzlin, S.; Siepmann, J. *Int. J. Pharm.* **2006**, *314*, 198.
12. Liu, Y.; Schwendeman, S. P. *Mol. Pharmaceutics* **2012**, *9*, 1342.
13. Fu, K.; Pack, D. W.; Klibanov, A. M.; Langer, R. *Pharm. Res.* **2000**, *17*, 100.
14. Brunner, A.; Mäder, K.; Göpferich, A. *Pharm. Res.* **1999**, *16*, 847–853.
15. Ford Versypt, A. N.; Pack, D. W.; Braatz, R. D. *J. Control. Release* **2013**, *165*, 29.
16. Sansdrap, P.; Moës, A. J. *J. Control. Release* **1997**, *43*, 47.
17. Siparsky, G. L.; Voorhees, K. J.; Miao, F. D. *J. Environ. Polym. Degrad.* **1998**, *6*, 31.
18. Antheunis, H.; van der Meer, J. C.; de Geus, M.; Kingma, W.; Koning, C. E. *Macromolecules* **2009**, *42*, 2462.
19. Antheunis, H.; van der Meer, J. C.; de Geus, M.; Heise, A.; Koning, C. E. *Biomacromolecules* **2010**, *11*, 1118.

ID: jwweb3b2server Time: 13:01 I Path: D:/Wiley/Support/XML_Signal_Tmp_AA/JW-APP#170615

J_ID: z8e Customer A_ID: APP45464 Cadmus Art: APP45464 Ed. Ref. No.: 20170772 Date: 7-July-17 Stage: Page: 9

20. Nishida, H.; Yamashita, M.; Nagashima, M.; Hattori, N.; Endo, T.; Tokiwa, Y. *Macromolecules* **2000**, *33*, 6595.
21. Lyu, S. P.; Schley, J.; Loy, B.; Lind, D.; Hobot, C.; Sparer, R.; Untereker, D. *Biomacromolecules* **2007**, *8*, 2301.
22. Wang, Y.; Pan, J. Z.; Han, X. X.; Sinka, C.; Ding, L. F. *Biomaterials* **2008**, *29*, 3393.
23. Han, X. X.; Pan, J. Z. *Biomaterials* **2009**, *30*, 423.
24. Soares, J. S.; Zunino, P. *Biomaterials* **2010**, *31*, 3032.
25. Chen, Y.; Zhou, S.; Li, Q. *Acta Biomater.* **2011**, *7*, 1140.
26. Casalini, T.; Rossi, F.; Lazzari, S.; Perale, G.; Masi, M. *Mol. Pharmaceutics* **2014**, *11*, 4036.
27. Busatto, C.; Berkenwald, E.; Mariano, N.; Casis, N.; Luna, J.; Estenoz, D. *Polym. Degrad. Stab.* **2016**, *125*, 12.
28. Sah, H. J. *Control. Release* **1997**, *47*, 233.
29. Park, T. G. *J. Control. Release* **1994**, *30*, 161.
30. Fitzgerald, J. F.; Corrigan, O. I. *J. Control. Release* **1996**, *42*, 125.
31. Wang, H. T.; Palmer, H.; Linhardt, R. J.; Flanagan, D. R.; Schmitt, E. *Biomaterials* **1990**, *11*, 679.
32. Hakkarainen, M.; Albertsson, A. C.; Karlsson, S. *Polym. Degrad. Stab.* **1996**, *52*, 283.
33. Vey, E.; Roger, C.; Meehan, L.; Booth, J.; Claybourn, M.; Miller, A.; Saiani, A. *Polym. Degrad. Stab.* **2008**, *93*, 1869.
34. Hagberg, J.; Düker, A.; Karlsson, S. *Chromatographia* **2002**, *56*, 641.
35. Ford, A. N.; Pack, D. W.; Braatz, R. D. *Comput.-Aided Chem. Eng.* **2011**, *29*, 1475.
36. Dunne, M.; Corrigan, O. I.; Ramtoola, Z. *Biomaterials* **2000**, *21*, 1659.
37. Raman, C.; Berkland, C.; Kim, K.; Pack, D. W. *J. Control. Release* **2005**, *103*, 149.

ID: jwweb3b2server Time: 13:01 I Path: D:/Wiley/Support/XML_Signal_Tmp_AA/JW-APP#170615

SGML and CITI Use Only
DO NOT PRINT